Philosophical Magazine

ISSN: (Print) (Online) Journal homepage: https://www.tandfonline.com/loi/tphm20

The role of electric current in the formation of white-etching-cracks

P.-Y. Tung , E. McEniry & M. Herbig

To cite this article: P.-Y. Tung , E. McEniry & M. Herbig (2020): The role of electric current in the formation of white-etching-cracks, Philosophical Magazine, DOI: 10.1080/14786435.2020.1819578

To link to this article: https://doi.org/10.1080/14786435.2020.1819578

Published online: 18 Sep 2020.

PHILOSOPHICAL MAGAZINE
https://doi.org/10.1080/14786435.2020.1819578

Taylor & Francis
Taylor & Francis Group

The role of electric current in the formation of white-etching-cracks

P.-Y. Tung[a], E. McEniry[b] and M. Herbig[a]

[a]Department of Microstructure Physics and Alloy Design, Max-Planck-Institut für Eisenforschung GmbH, Düsseldorf, Germany; [b]Department of Computational Materials Design, Max-Planck-Institut für Eisenforschung GmbH, Düsseldorf, Germany

ABSTRACT

Material failure by white-etching-cracks (WECs) can cause enormous economic costs. The formation of WECs emerges from the decomposition of the original, usually cementite-containing, microstructure. As small amounts of electric current can trigger this failure mechanism, we investigate the contribution of electric current to cementite decomposition. We applied ~700 A/cm^2 for two weeks at 60°C to a pearlitic Fe-0.74C (wt%) specimen. The comparison of the microstructure before and after showed no differences. Theoretical considerations support the conclusion that at this low temperature such electric current densities cannot directly cause cementite decomposition. Electric current could play an indirect role in the formation of WECs, however, by generating hydrogen from the lubricant which is known to accelerate WECs formation.

ARTICLE HISTORY
Received 12 June 2020
Accepted 31 August 2020

KEYWORDS
Cementite decomposition; electricity; electromigration

Introduction

White-etching-cracks (WECs) are a failure phenomenon occurring in high carbon steels subjected to intense mechanical loads. In direct vicinity to WECs, pronounced microstructural changes are observed. The original microstructure decomposes and transforms into nanocrystalline ferrite. These regions are called white-etching-areas (WEAs) according to their bright appearance after etching in the light microscope. The coupling of WECs/WEAs is primarily reported to occur in bearings and rails but also concerns many further widespread engineering applications such as washing machines, transmissions, dryers and many more [1,2]. Material failure by WECs is thus a ubiquitous phenomenon causing enormous economic costs world-wide. The formation of WECs and concurrent WEAs is affected by complex interactions between

CONTACT P.-Y. Tung p.tung@mpie.de Department of Microstructure Physics and Alloy Design, Max-Planck-Institut für Eisenforschung GmbH, Max-Planck-Str. 1, Düsseldorf 40237, Germany

multiple parameters, such as (but not limited to) deformation, temperature, electric current, lubrication conditions, and material types. As a result, depending on the operation conditions and/or types of steels, WECs can be generated in different ways. For example, in the case of rails, due to elevated temperature and higher lateral shear forces, WEAs (in this field usually called white-etching-layers, WELs) form on the surface before crack initiation occurs in the WELs or at the interface to the base material [3]. WEAs can also be generated by cyclic heating alone [4], or by adiabatic heating due to ballistic impact [5]. Although the formation conditions might be very different, all WEAs/WELs have in common that the original microstructure consisting of martensite (or ferrite) and cementite decomposes and transforms into ferritic grains encompassed by carbon grain boundary segregation [6]. Here, we focus on the occurrence of this failure phenomenon in bearings where mainly the steel 100Cr6 consisting of martensite and cementite is employed. Although the formation mechanism of WECs/WEAs in 100Cr6 is still debated, a recent study showed that WEAs could form by intense mechanical mixing within a few nm around the moving WECs [7]. The mechanical decomposition of the ~1 μm sized spherical cementite precipitates in 100Cr6 with a nanohardness of 15.1 GPa [8] is the hardest obstacle that needs to be overcome in this process. These indicate that, to form WEAs, it is necessary to decompose large spherical cementite precipitates. Then, the carbon released from the decomposed cementite segregates to the ferrite grain boundaries what stabilized the nanocrystalline grain size [9]. Thus, cementite decomposition and the release of its carbon content into the matrix plays a crucial role for the formation of WECs/WEAs.

Electric current is reported to trigger early WEC-induced failure of bearings in laboratory experiments [6,10]. The flow of electric current cannot be completely avoided in bearings for electrical applications [11]. The non-conductive lubricant between bearing balls and bearings acts as a dielectric material, and friction between the thereby electrically insulated bearing parts or insufficiently insulated electric parts in the surrounding may lead to electrostatic surface charging. Once the electric field exceeds the disruptive strength of the lubricant, electrical discharges occur and electric current flows across the non-conductive lubricant film through the bearing [6,10]. It is well-known that the flow of electric current through a material can affect its microstructure and properties. This can occur in multiple ways. Firstly, electric current can influence the thermodynamic equilibrium of a material system. The passage of current flow provides extra free energy to the system, promoting the structure towards a state with overall lower electrical resistance to minimise the overall system free energy [12]. Following a similar principle, passing high electric current pulsing (ECP) on drawn pearlitic wire is able to compensate the increment of interfacial energy and achieve microstructure refinement [13], improving the deformability. Secondly, electric current increases a material's temperature due to the friction of the moving electrons (electric Joule heating). Cracks

within medium carbon steels can be partly healed under ECP due to this effect [14]. Thirdly, electrons moving through a material exert a momentum transfer onto the atoms they collide with (electric wind force). This causes directional diffusion of atoms, so-called electromigration, and can potentially affect the movement of dislocation [15]. For high current densities at elevated temperatures, this phenomenon has been shown to be able to alter the carbon distribution in both austenite [16] and ferrite [17]. Furthermore, flash marks on the surface of bearings can be created by infrequent high-current-induced arcing [18,19].

However, all the electric effects described above have been reported only at current densities above 2,000 A/cm^2, or at temperatures above 500°C. In standard bearings, temperatures remain below 100°C and regulations instruct that current densities be kept below 10 A/cm^2 [20,21] or 9 A/cm^2 [22] as flash marks are created at current densities down to 70 A/cm^2 [23]. Yet as shown in Loos' experiments [6], WECs were triggered at a current density of 5×10^{-3} A/cm^2, well below this threshold. It must therefore be assumed that electric stray currents occurring in service might be a crucial ingredient for the formation of this failure mechanism in practice.

Nonetheless, the underlying mechanism how electric currents provoke WECs is still unknown. As mentioned, the largest obstacle of generating WECs/WEAs in 100Cr6 is the decomposition of cementite. Since electric current triggers WECs formation, it must help overcome this obstacle, i.e. it must induce cementite decomposition. This can either be a direct effect caused by the motion of electrons through the material or by indirect effects such as by the generation of hydrogen from the lubricant which then promotes the microstructure decomposition required for WECs formation. The latter is a plausible scenario, as hydrogen is known to trigger WEC formation in bearings [2] and as it can be generated from the lubricant employed in bearings by electric discharge events [24]. Therefore, it must be clarified if electric current triggers the formation of WECs directly via the decomposition of carbides, or indirectly via other interactions, such as the generation of hydrogen from the lubricant.

The experiments Loos et al. [6] performed, were conducted on the complex microstructure of a technical alloy, involving rolling contact deformation, electric current and lubrication. This complexity makes it difficult to understand the contribution of the individual parameters to the failure phenomenon. To better understand the influence of electric current itself, we simplify the system and investigate only in how far low-density electric currents applied for an extended period can lead to the decomposition of cementite in a binary Fe-C pearlitic steel at a fixed operating temperature and excluding all other factors such as deformation and lubricant. We use a custom-designed experimental set-up to apply a controlled current density at constant temperature and compare the microstructure before and after by electron channelling contrast imaging (ECCI). Further, we use theoretical considerations and simulations to discuss the

possible role of electric current for the decomposition of carbides in undeformed and deformed pearlite.

Experimental methods

To emphasise the effect of electric current on carbide decomposition, we choose a hypoeutectoid binary pearlitic steel with the composition of Fe-0.74C (wt.%). The steel was cast into a rectangular crucible mould, hot-rolled to 90% thickness reduction at 1150°C, and air-cooled to room temperature. It was homogenised at 1000°C for 4 h in argon atmosphere, followed by rapid-cooling to 575°C by a direct contact to a Cu-plate in a preheated furnace. Here, it was held for 5 min where pearlite formation occurred and then quenched in oil. This treatment leads to a microstructure consisting of fine cementite lamellae which is especially prone to decomposition.

To investigate the influence of electric current on the decomposition of cementite, a simple direct current circuit was established as shown in Figure 1. An electrical resistance was employed to better control the current density. Initially, a current density of 672 A/cm² was applied along the length axis of a sample with a geometry of 9 mm × 1 mm × 0.5 mm in a temperature-controlled room at 23°C. The electric resistivity heating led to a sample temperature of 60 ± 0.5° C, measured using a PT-100 resistance thermometer. Contact point oxidation led to a continuous increase of the system's resistivity during the two-week long experiment. To compensate for this effect and thus to maintain the temperature at exactly 60°C, the current density was gradually increased to 773 A/cm². The test conditions are listed in Table 1. In order to clarify the role of electric current, rather than directly taking the parameters from Loos' experiments [6], significantly more severe test conditions were applied. Higher current density (~700 A/cm²) and longer exposure time (336 h) were used. However, no mechanical load was applied in the case investigated here.

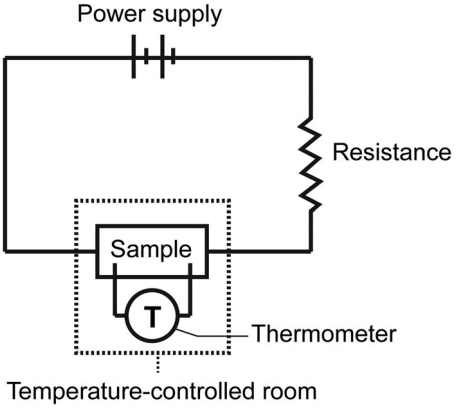

Figure 1. Circuit diagram of the experimental setup.

Table 1. Test conditions in this work and in Loos' [6] work for comparison.

Material	Current density	Time	Temperature	Geometry of carbide	Load
Fe-0.74C	672–773 A/cm^2	336 h	60°C	lamellae (~50 nm)	–
100Cr6 [6]	~5×10^{-3} A/cm^2	200 h	100°C	round (~1 µm)	1900–2400 N/mm^2

Microstructure characterisation was carried out on the sample before and after the electric current experiment. To retrieve the same position before and after the experiment, a 15 µm × 15 µm micro indention mark was made on the surface. ECCI was conducted in a Zeiss Merlin field emission gun-scanning electron microscope (FEG-SEM) with a voltage of 30 kV and a working distance of 7.5 mm.

Results

As mentioned, the main focus of this study is to isolate the effects of electric current from a complex interaction of different parameters (e.g. deformation, lubricant, and microstructure). To better understand the influence of electric current itself, we chose to simplify the experimental conditions as far as possible. Therefore, we only employ continuous electric current on a binary pearlitic steel, and thereby exclude the effects of electric current itself on the formation of WEAs/WECs.

Figures 2 and 3 show ECCI micrographs of the microstructure before and after exposure to electric current. In both cases, the current was applied for two weeks with a current density of 672–773 A/cm^2. In the case of Figure 2 the cementite lamellae are oriented in the direction of the current flow, in Figure 3 the lamellae are oriented 45° with respect to the current flow. Between the exposure to electric current and the second ECCI measurement the specimen had to be slightly polished to remove the surface oxide layer. Thus, the ECCI micrographs before and after do not show exactly the same location. Nevertheless, the imaging locations are close enough together to allow good comparison.

Before the current passage (Figure 2), the cementite lamellae show up as elongated features in bright grey. The surrounding ferrite appears either bright or dark. The pronounced intensity variations in ferrite are due to the strong dependence of the ECCI contrast on grain orientations of about 0.3° [25,26]. Small misorientations or slight distortions in the crystal lattice strongly influence the contrast. Pearlitic ferrite is known to contain orientation gradients, also within individual colonies [27], and this causes alternating dark and bright ferrite blocks in the ECCI micrographs (Figure 2). The bright lines visible in ferrite represent dislocations. The high orientation sensitivity of the image contrast in ECCI means that the contrast in the micrographs before and after exposure to electric current can appear significantly different. In practice, it is difficult to place the sample with an angular accuracy below 0.3°. As a result,

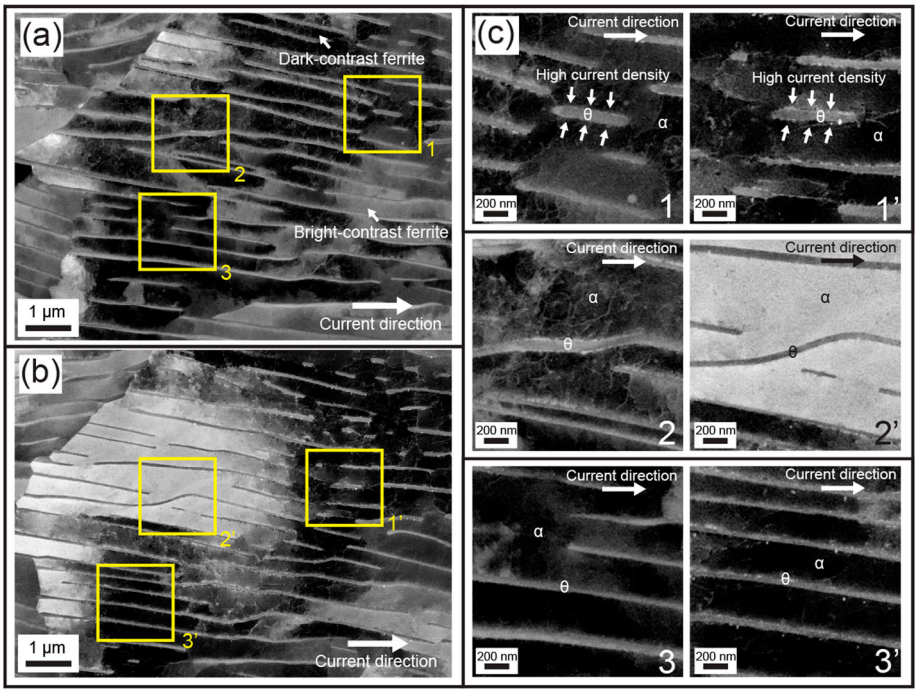

Figure 2. ECCI micrographs of cementite lamellae before and after exposure to electric current. Case: Alignment of lamellae parallel to the macroscopic current flow direction. Low-resolution images before (a) and after (b) exposure to electric current. The yellow squares labelled 1,2,3 mark subregions that are shown at higher magnifications in (c). Note that the images before and after do not show exactly the same location as the specimen was polished in between. The strong contrast changes in the ferritic matrix before and after is due to the high orientation sensitivity of ECCI, not to influences by electric current. No signs of cementite decomposition by electric current such as thinning or rounding of edges are observed.

slight contrast changes cannot be entirely avoided. However, viewing a specimen from slightly different orientations by ECCI affects here only the contrast of the cementite, ferrite and lattice defects. The morphology of the cementite lamellae is hardly affected by small tilting angles and thereby a comparison of the morphology before and after is possible.

Current densities will distribute inhomogeneously in ferrite and cementite. At room temperature, the electrical resistivity of pure cementite is $\sim 6.7 \times 10^{-5}$ Ω·cm [28,29]. This is about 4 times higher than the one of pure ferrite which is $\sim 1.5 \times 10^{-5}$ Ω·cm [28–30]. Once electric current runs through a pearlitic microstructure, the current density in ferrite will thus be higher than in cementite. The highest local current density levels are present in areas where electrons travelling through ferrite meet the edge of a cementite lamella and are forced to diverge to pass it. This leads to a local temperature increase at these locations which may also result in local thermal stresses. According to simulations [31], the associated thermal expansion can be high enough to cause local decomposition of cementite. However, a rather high current density of 1×10^6 A/cm^2

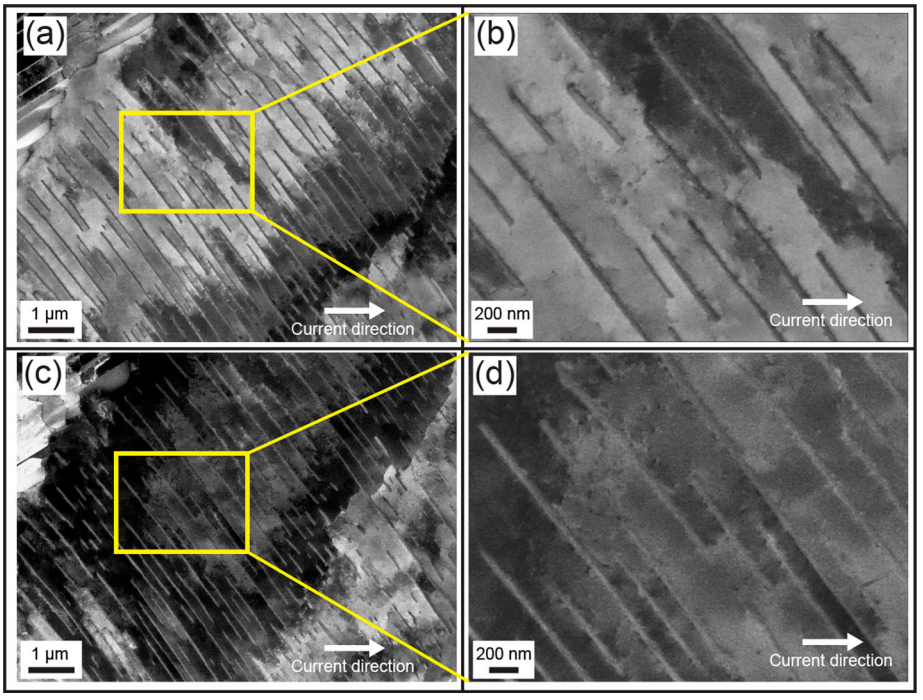

Figure 3. ECCI micrographs of cementite lamellae before and after exposure to electric current. Case: Alignment of lamellae at 45° with respect to the macroscopic current flow direction. (a) Low-resolution and (b) high resolution image before exposure to electric current. (c) Low-resolution and (d) high resolution image after exposure to electric current. Note that the images before and after do not show exactly the same location as the specimen was polished in between. The strong contrast changes in the ferritic matrix before and after is due to the high orientation sensitivity of ECCI, not to influences by electric current. No signs of cementite decomposition by electric current such as thinning or rounding of edges are observed.

with an impulse time of 100 µs must be applied [31] to trigger this effect, and thereby this scenario can be excluded in the current case.

Nevertheless, the faces of cementite lamellae are the regions exposed to the highest local current densities. If electric current is able to decompose cementite under the given conditions this effect should be most pronounced and most clearly visible at these locations. Such locations are marked in the Figure 2 by white arrows. Here, a cementite lamella starts in the ferrite and the electrons coming from the left will bifurcate to bypass it, thereby creating a zone of locally increased current density directly next to the precipitate. After exposure to electric current (Figure 2), however, the overall pearlitic microstructure shows no substantial changes. Figure 2 shows magnifications of subregions from Figure 2(b). No clues for cementite decomposition, such as thinning of cementite or rounding of edges, were found.

Figure 3 shows ECCI micrographs of a region where the cementite lamellae were inclined 45° with respect to the macroscopic current flow direction before (Figure 3) and after (Figure 3) exposure to the same electric conditions

as before. As before, the microstructure shows no current-related changes: the geometry of lamellae remains sharply straight and neither thickness reduction nor fragmentation of cementite lamellae is observable.

Discussion

Role of electric current in case of undeformed pearlite

Electric current is known to trigger failure by WECs [6]. The formation of WECs involves the decomposition of the original microstructure consisting of martensite and cementite and its transformation into ferritic grains encompassed by carbon grain boundary segregation [9]. In this process, the decomposition of cementite is the most difficult part, due to the high hardness of this phase and because the emission of the carbon content of cementite into martensite or ferrite is an energetically unfavoured act [8]. This raises the question to what extent electric current causes or aids the decomposition of cementite. As shown in Table 1, in Loos' experiments, a current density of $\sim 5 \times 10^{-3}$ A/cm² was applied for 200 h at 100°C in 100Cr6 steel. To be able to see a clear effect of electric current on cementite decomposition, significantly more severe conditions were applied in this work. The current density we used here was 5 orders of magnitude higher, the exposure time to electric current was almost 70% longer, while the temperature was similar. Further, the composition of cementite investigated in this study was particularly selected to be less stable and hence easier to be decomposed than the cementite present in the 100Cr6 steel investigated by Loos et al. Cementite is a metastable phase and Cr and Mn are able to reduce its formation enthalpy [32]. In 100Cr6, the typical Cr-rich cementite contains about 12 at. % Cr, which reduces cementite formation energy by $\sim 5 \times 10^{-3}$ eV/atom [33]. As a result, the thermodynamic stability of the binary Fe-C cementite used for this work is thus lower than the one of the Cr-rich cementite in 100Cr6. Furthermore, the size and shape of cementite in our sample was adjusted for easier decomposition. The ~50 nm thick lamella used here have a much higher surface to volume ratio than the ~1 µm round cementite in 100Cr6 and should thus be more prone to decomposition. Further, the tip of cementite lamellae has a curvature radius of ~20 nm which enhances the decomposition due to the Gibbs-Thompson effect [34–36]. All of the conditions mentioned above should make the system investigated here more prone to decomposition than the 100Cr6 in the experiments of Loos. Thus, if no obvious cementite decomposition is observed in our experiments, it can be excluded that electric current alone, without the additional presence of plastic deformation, can decompose cementite particles in 100Cr6.

In order to further validate these experimental results, we consider the energetics of the decomposition process of cementite by electric current. For this, we consider the entire cementite decomposition process as the transportation of

carbon from cementite to ferrite through the interface. For this process to occur, a carbon atom has to run through different locations and energy states: First, it must leave its stable position in the first atomic layer of cementite to occupy an interstitial lattice site in cementite. Next, it must pass the cementite / ferrite interface. Finally, it must relocate to an octahedral site in ferrite. This overall process involves an energy barrier. For cementite decomposition to take place, the carbon atoms must acquire an energy larger than this energy barrier. This barrier was calculated using the standard nudged-elastic band technique which was originally developed for the evaluation of diffusion barriers. The energetics of the system were assessed using the environmental tight-binding approach of McEniry et al. [37,38]. For the calculation it was assumed that cementite and ferrite have a Bagaryatski orientation relationship, and that cementite has the stoichiometric carbon content of 25 at.%. According to these calculations, the activation barrier required to move a carbon atom from the outermost layer of cementite across the cementite-ferrite interface into the first atomic layer of ferrite is 2.17 eV. Much of this large activation energy is related to the very low solubility of carbon in ferrite.

Next, we will discuss if and how electric current could help to overcome this energy barrier. As mentioned in the previous section, the applied current has two main effects that could potentially influence the carbon migration behaviour: electric Joule heating and electromigration. Joule heating results from inelastic energy transfer between the moving electrons and vibrating atoms. In our case, we applied a current density of ~700 A/cm^2 through the sample and carefully regulated the overall temperature to maintain 60°C (333 K) by slightly increasing the current density throughout the two weeks of experiment. For a given Energy barrier $E_{\text{barrier}} = 2.13$ eV, the carbon hopping frequency ν at the temperature $T = 333$ K can be estimated by

$$\nu = \nu_0 \exp(-\frac{E_{\text{barrier}}}{kT}), \tag{1}$$

where ν_0 is the attempt frequency and k is the Boltzmann constant. By taking $\nu_0 = 1.2 \times 10^{13}\,\text{s}^{-1}$ [39], we obtain $\nu = 6.94 \times 10^{-20}\,\text{s}^{-1}$. Clearly, at the average specimen temperature of 333 K, it is almost impossible for carbon to jump from cementite to ferrite. However, local Joule heating will lead to local temperature increase around cementite. From Ref. [31], the authors estimated that the maximum local temperature increment of current flowing is approximately 60 K immediately after a 100-μs-long current impulse with a current density of 1×10^6 A/cm^2 through a spherical cementite in ferrite. The current density used for these simulations is three orders of magnitudes higher than in our case. Thus, local peak temperatures in our case will be certainly below 60 K and this justifies using 60 K as upper bound for the local temperature increment.

At an average sample temperature of 60°C and assuming a local temperature increment of 60°C at locations with the highest current density, local peak temperatures would reach 120°C. This would result in a hopping frequency for carbon of $5.8 \times 10^{-15} s^{-1}$. Even at this hopping frequency it would take 5.5 million years for a single carbon atom to leave cementite. A typical cementite lamella has a dimension of 50 nm × 1 μm × 1 μm, a cementite unit cell has a size of 0.50 nm × 0.67 nm × 0.45 nm and contains 4 carbon atoms and thus each cementite lamella contains about 1.3×10^9 C atoms. These numbers make clear that at the applied current density, despite assuming the highest possible local temperatures, the effect of Joule heating is far too low to trigger carbide decomposition.

A second possibility how electric current could aid the decomposition of cementite is electromigration. The electromigration force exerted on a single carbon atom is given by:

$$F_{\text{electromigration}} = Z^* e \rho j, \tag{2}$$

Where e is the elementary charge, ρ is the resistivity, j is the current density, and Z^* refers to the effective charge number. Using a semi-classical ballistic model of scattering [40] and experimental parameters, Hideo derived an approximate equation [17]:

$$Z^* = 3110 \frac{\Delta \rho_d}{\rho}, \tag{3}$$

where $\Delta \rho_d$ is the resistivity increment in the alloy due to the existence of carbon and ρ is the alloy resistivity. Due to the correlation between $\Delta \rho_d$ and ρ and temperature, Z^* is a temperature-dependent parameter. From Hideo's work [17], Z^* is 12.2 at 550°C in ferrite, and it reduces to 4.4 at 700°C. Z^* is unknown out of the range of 550–700°C, so we extrapolate it to be 38 at 60°C by assuming a linear dependence of Z^* on temperature. With the resistivity of cementite $\rho = 6.7 \times 10^{-7}\ \Omega \cdot \text{m}$ and $\bar{j} = 0.07\ \text{A} \cdot \text{m}^{-1}$ this results in an electromigration force for C in cementite of 1.77×10^{-6} eV·Å^{-1}. To assess in how far this force might play a role for the movement of carbon in cementite, we compare it to the atomic vibration forces of pure carbon in the form of diamond. At a typical atomic vibration amplitude $\sim 10^{-11}$ m [41] and a force constant 60.9 N·m^{-1} [42], the maximum atomic vibration force of diamond is 3.81×10^{-1} eV·Å^{-1}. As this is about 5 orders of magnitude higher than the electromigration force calculated above we conclude that under the given electric and temperature condition the influence of electromigration on the decomposition of cementite is negligible.

Furthermore, the electromigration force on carbon could be much lower than what we calculate due to the overestimation of current density used for the calculations with equation (2). WECs initiate below the surface in a depth of around 100 μm and here the current density will be significantly lower than

the externally applied current density. The interior electric field, which is induced by the large capacitance between bearing balls and bearing surface, will affect the distribution of current density in bearings. Rather than evenly running through the material, the electrons will immediately distribute on the surface to compensate the interior electric field. As a consequence, at the depth of several hundreds of micrometers, where WECs initiate, the current density will be much lower than that on the surface.

There are further effects which make C decomposition even more difficult. The removal of a C atom from cementite activates three counter mechanisms which act against the further decomposition process. With each removed C atom the surrounding ferrite gets more supersaturated with C which states an energetically unfavoured condition. Moreover, when a carbon atom leaves cementite, a carbon vacancy is left behind. The migration barrier for carbon diffusion via a vacancy in cementite is 1.99 eV [43], which makes vacancy movement difficult in cementite. The vacancy remains close to the interface where it constitutes a very significant trap for any further decomposition events. Finally, the presence of a carbon vacancy in cementite makes the extraction of a second carbon atom in the direct vicinity even more difficult. Thus, with each carbon atom transferred from cementite to ferrite it gets increasingly difficult to continue the decomposition process.

In summary, even if the electrically-assisted transfer of C from cementite to ferrite might happen from time to time, this would be a rare event. However, to decompose larger quantities of cementite large numbers of C atoms need to be transferred, which is exceptionally unlikely under the present conditions. Therefore, current-induced cementite decomposition, in the absence of additional external forces, is highly implausible unless much higher local current densities than employed here are reached. The experimental observations are in agreement with theoretical assessments. We conclude that it is impossible to decompose undeformed cementite using current densities of ~700 A/cm² at 60°C. Based on this insight, we can exclude that cementite decomposition occurs by a direct effect of electric current in the case of 100Cr6 bearings where much lower current densities are applied and which are less prone to decomposition due to their morphology and composition.

The role of electric current in case of deformed pearlite

In the previous section, only undeformed pearlite was considered. However, bearings are subjected to high mechanical loads and plastic deformation, which are known to cause cementite decomposition [9,34,44–48]. In Loos' experiments, in addition to electric current, a rolling contact load of 1900–2400 N/mm² was applied on the 100Cr6 bearing. This caused severe plastic deformation due to Hertzian contact stresses [49] in the zone where WECs initiate, i.e. within the first hundred micrometers of depth below the raceway surface. Ideally, the same experiments as described above should be

carried out also on deformed pearlite to investigate the role of electric current on cementite decomposition experimentally. However, for practical reasons this was not possible. After exposure to electric current, the specimen must be polished to remove the surface oxide layer in order to attain high quality ECCI micrographs. This makes it impossible to investigate exactly the same location before and after exposure to electric current. Plastic deformation leads to pronounced local differences of grain orientations and cementite morphology. The microstructure of deformed pearlite thus appears too different to be compared even if only a few hundred nanometres are removed by polishing. This makes it impossible to compare the microstructure before and after applying electric current. However, also by theoretical reasoning, it can be excluded that the current flow has a significant effect in the case of deformed pearlite, as detailed below.

Carbon transport by electric current is entirely different when comparing the scenarios deformed and undeformed cementite. As mentioned in the prior section, for undeformed cementite, removal of carbon from cementite to ferrite involves overcoming a high energy barrier, and therefore hardly takes place under our experimental condition. In the case of heavily deformed cementite, this energy barrier is already overcome as plastic deformation alone is already sufficient to remove carbon from cementite. Carbon will be transferred from cementite into ferrite by the solute drag effect, where dislocations that intersect the cementite carry carbon into ferrite [48,50]. This is because the binding energy of carbon in cementite is lower than the one of carbon to dislocations in ferrite [48,51–53]. Further, the mechanically induced fragmentation of cementite increases the free energy difference between cementite and ferrite, which increases the solubility of carbon in ferrite near the interface; a phenomenon known as the Gibbs-Thompson effect [34,35]. Clearly, even without the influence of electric current, severe plastic deformation itself is sufficient for cementite decomposition, and this has been shown in numerous studies on cold-drawn pearlitic wires [34,45–47].

It remains to be clarified if small amounts of electric current can significantly accelerate the process of cementite decomposition that naturally occurs when pearlite is exposed to severe plastic deformation. As it is hardly possible for electric current to transfer carbon from cementite to ferrite, we assume that this transfer is only mediated by plastic deformation. Assuming that, the only possible way how electric current could accelerate the process of cementite decomposition is by accelerating carbon diffusion in ferrite. Accelerated diffusion would speed up the redistribution of C in ferrite, thereby lowering the amount of C supersaturation in ferrite in direct vicinity of cementite, which renders it less difficult for the next C atom to leave cementite. We therefore consider the influence of electric current on the carbon flux in ferrite. As described above, electromigration provides a driving force to bias the carbon diffusion behaviour. The carbon diffusion flux can be determined by a modified version of Fick's

first law:

$$\vec{J}_c = \frac{D_c C_c}{kT}\left(\nabla \mu_c + |Z^*|e\rho\vec{j}\right), \tag{4}$$

where $\vec{J}_c$ is the carbon flux, D_c is the carbon diffusivity, C_c is the carbon concentration, and $\nabla\mu_C$ is the chemical potential gradient of carbon. The carbon diffusion flux is mainly affected by the change of diffusivity D_c and the term for the electric current $|Z^*|e\rho\vec{j}$ which acts as a driving force here. Similar to the calculation above, with the resistivity of ferrite 1.5×10^{-5} Ω·cm and an applied current density of 700 A/cm^2, an electromigration force for carbon in ferrite $|Z^*|e\rho\vec{j} = 1.05 \times 10^{-7}$ eV·Å^{-1} is obtained. Compared to the chemical potential gradient of carbon between two nearest octahedral sites $\nabla\mu_C \cong 0.18$ eV·Å^{-1}[39], the contribution of $|Z^*|e\rho\vec{j}$ in equation (4) is thus negligibly small.

Furthermore, in a deformed ferrite lattice, diffusion of carbon atoms would already be significantly enhanced by lattice strain (or residual stresses). According to simulations [39] and experimental results [54], the carbon diffusion barrier between interstitial sites is ~0.86 eV in an undistorted ferrite lattice. However, the diffusion energy profile is significantly altered in the stress field of dislocations. The carbon diffusion barrier drops to ~0.2 eV in the vicinity of a screw dislocation [39], indicating that carbon is very mobile in the neighbourhood of the screw dislocation centre. Therefore, in the case of highly deformed ferrite containing high amounts of dislocations, carbon diffusion is already enhanced due to the reduction of the diffusion barrier by the elastic stress field of dislocations. Compared to this effect, the contribution of electric current can be considered as marginal.

Clearly, the influence of electric current at these current densities is not sufficient to significantly alter carbon diffusion behaviour. Rather, the main transport of carbon would be caused by solute drag by dislocations, and also this would be an effect caused by severe plastic deformation, not by electric current.

Possible indirect role of electric current for triggering WECs in bearings

We have shown that the small amounts of electric current used to provoke the formation of WECs under laboratory conditions without deformation cannot decompose cementite. Plastic deformation alone, in absence of electric current, is known to be able to decompose cementite [48,51–53] and, as shown above, the additional application of electric current on plastically deformed cementite has only a negligible effect on the acceleration of this process. So, a direct effect of electric current leading to premature microstructure decomposition can be excluded and indirect effects must be presented. The experiments conducted by Loos et al. that lead to premature failure by WECs involved multiple influence parameters consisting of deformation, electric

current and lubricant. Thus, a combined effect of these parameters is plausible, such as an interaction between electric current and lubricant. Electric current is known to cause thermal dissociation of lubricants, resulting in the formation of hydrogen cations [6]. Lubricants usually have very low electrical conductivity and can be thus considered as insulators in bearings running at full-film lubrication conditions. When a direct electric current is applied at a bearing the bearing parts act as condensers and accumulate charge. In service, such charges can arise from friction-induced electrostatic charging of the rolling elements or from insufficiently insulated electric parts in the surrounding. When the avalanche voltage of the lubricant is reached, an electric discharge event takes place. This creates a plasma in the lubricant that cracks the lubricant partly into hydrogen [2]. Then, positively charged hydrogen is absorbed on the cathodic steel surface before diffusing into the material. Hydrogen is known to enrich in bearings that show WECs failure during application [55]. It is also known to be trapped in zones of high residual stresses in steels [55,56]. In bearings, hydrogen would thus be expected to be trapped in the zone of the highest Hertzian stresses. This is usually in about 100 µm depth below the bearing raceway surface and this is also the zone where WECs initiate. In this zone, hydrogen would enrich at dislocations and interfaces [57,58] where it would simplify plastic deformation according to the hydrogen enhanced local plasticity (HELP) effect [59] and the formation of cracks according to the hydrogen enhanced decohesion (HEDE) effect [60]. It can be assumed that the HELP effect also simplifies the mechanical decomposition of cementite which is a prerequisite for WECs formation and thereby triggers this failure phenomenon. However, this point requires further clarification.

Conclusions

- In this work, a hypoeutectoid pearlitic steel with the composition of 0.74 wt.% was observed before and after being exposed to a current density of ~700 A/cm² at 60°C. Based on ECCI characterisation, the comparison of microstructures shows no obvious changes related to electric current.
- Theoretical considerations confirm: At such low amounts of electric current and temperatures cementite decomposition does not take place as the resulting electromigration force and local temperature increments are not high enough to overcome the high energy barrier for carbon migration from cementite to ferrite.
- We conclude that electric current most likely plays an indirect role in the formation of WECs, supposedly, by interacting with the lubricant and generating hydrogen, which is known to accelerate WECs formation.

Acknowledgement

The authors acknowledge funding by the German Federal Ministry of Education and Research (BMBF) through grant 03SF0535. P.-Y. Tung acknowledges financial support by the International Max Planck Research School for Interface Controlled Materials for Energy Conversion (IMPRS-SurMat). The authors acknowledge the support of Iván González concerning the experimental setup.

Disclosure statement

No potential conflict of interest was reported by the author(s).

Funding

This work was supported by Bundesministerium für Bildung und Forschung [grant number 03SF0535]; International Max Planck Research School for Interface Controlled Materials for Energy Conversion.

References

[1] M.H. Evans, L. Wang, and R.J.K. Wood, *Formation mechanisms of white etching cracks and white etching area under rolling contact fatigue*. Proc. Inst. Mech. Eng. J. J. Eng. Tribol. 228 (2014), pp. 1047–1062.
[2] M.H. Evans, *An updated review: white etching cracks (WECs) and axial cracks in wind turbine gearbox bearings*. Mater. Sci. Technol. 32 (2016), pp. 1133–1169.
[3] A. Kumar, G. Agarwal, R. Petrov, S. Goto, J. Sietsma, and M. Herbig, *Microstructural evolution of white and brown etching layers in pearlitic rail steels*. Acta Mater. 171 (2019), pp. 48–64.
[4] J. Wu, R.H. Petrov, M. Naeimi, Z. Li, R. Dollevoet, and J. Sietsma, *Laboratory simulation of martensite formation of white etching layer in rail steel*. Int. J. Fatigue 91 (2016), pp. 11–20.
[5] Y. Xu, M. Umemoto, and K. Tsuchiya, *Comparison of the characteristics of nanocrystalline ferrite in Fe-0.89C steels with pearlite and spheroidite structure produced by Ball Milling*. Mater. Trans. 43 (2002), pp. 2205–2212.
[6] J. Loos, I. Bergmann, and M. Goss, *Influence of currents from electrostatic charges on WEC formation in rolling bearings*. Tribol. Trans. 59 (2016), pp. 865–875.
[7] L. Morsdorf, D. Mayweg, Y. Li, A. Diederichs, D. Raabe, and M. Herbig, *Moving cracks form white etching areas during rolling contact fatigue in bearings*. Mater. Sci. Eng. A 771 (2020), p. 138659.
[8] Y. Qin, J. Li, and M. Herbig, *Microstructural origin of the outstanding durability of the high nitrogen bearing steel X30CrMoN15-1*. Mater. Charact. 159 (2020), p. 110049.
[9] Y.J. Li, M. Herbig, S. Goto, and D. Raabe, *Atomic scale characterization of white etching area and its adjacent matrix in a martensitic 100Cr6 bearing steel*. Mater. Charact. 123 (2017), pp. 349–353.
[10] M. Zuercher, V. Heinzler, E. Schlücker, K. Esmaeili, T.J. Harvey, W. Holweger, and L. Wang, *Early failure detection for bearings in electrical environments*. Int. J. Cond. Monit. 8 (2017), pp. 24–29.
[11] H. Pittroff, *Waelzlager im elektrischen stromkreis*. Elektr. Bahnen 39 (1968), pp. 54–61.

[12] X. Zhang and R. Qin, *Exploring the particle reconfiguration in the metallic materials under the pulsed electric current*. Steel Res. Int. 89 (2018), p. 1800062.
[13] R. Qin, *Using electric current to surpass the microstructure breakup limit*. Sci. Rep. 7 (2017), p. 41451.
[14] Y. Zhou, J. Guo, M. Gao, and G. He, *Crack healing in a steel by using electropulsing technique*. Mater. Lett. 58 (2004), pp. 1732–1736.
[15] J.R. Lloyd, *Electromigration in integrated circuit conductors*. J. Phys. D Appl. Phys. 32 (1999), pp. 109–118.
[16] T. Okabe and A.G. Guy, *Steady-state electrotransport of carbon in iron*. Metall. Trans. 1 (1970), pp. 2705–2713.
[17] H. Nakajima and K.I. Hirano, *Electromigration of carbon in α-iron*. J. Appl. Phys. 48 (1977), pp. 1793–1796.
[18] H. Mikami and T. Kawamura, *Influence of electrical current on bearing flaking life*, 0148-7191, SAE Technical Paper, 2007.
[19] H. Prashad, *Tribology in Electrical Environments*, Elsevier, 2005.
[20] B. Pohrer, M. Zuercher, S. Tremmel, S. Wartzack, and E. Schlücker, *Einfluss des tribochemischen Schichtaufbaus auf die Ausbildung elektrisch induzierter Wälzlagerschäden*, Forschung und praktische Anwendungen, Tribologie-Fachtagung, Göttingen, Reibung, Schmierung und Verschleiß, 2015.
[21] S. Gruppe, *Stromisolierende Lager vermeiden Stromdurchgangsschäden*, Technische Produktinformation, Herzogenaurach, 2011.
[22] Y.-C. Chiou, R.-T. Lee, and C.-M. Lin, *Formation criterion and mechanism of electrical pitting on the lubricated surface under AC electric field*. Wear 236 (1999), pp. 62–72.
[23] H. Pietroff, *Wälzlager im elektrischen Stromkreis (Bearings in the electrical circuit)*. Elektr. Bahnen 3 (1968), pp. 54–61.
[24] K. Iso, A. Yokouchi, and H. Takemura, *Research work for clarifying the mechanism of white structure flaking and extending the life of bearings*, 0148-7191, SAE Technical Paper, 2005.
[25] I. Gutierrez-Urrutia, S. Zaefferer, and D. Raabe, *Electron channeling contrast imaging of twins and dislocations in twinning-induced plasticity steels under controlled diffraction conditions in a scanning electron microscope*. Scr. Mater. 61 (2009), pp. 737–740.
[26] S. Zaefferer and N.-N. Elhami, *Theory and application of electron channelling contrast imaging under controlled diffraction conditions*. Acta Mater. 75 (2014), pp. 20–50.
[27] T. Takahashi, D. Ponge, and D. Raabe, *Investigation of orientation gradients in pearlite in hypoeutectoid steel by use of orientation imaging microscopy*. Steel Res. Int. 78 (2016), pp. 38–44.
[28] M. Umemoto, Z.G. Liu, H. Takaoka, M. Sawakami, K. Tsuchiya, and K. Masuyama, *Production of bulk cementite and its characterization*. Metall. Mater. Trans. A 32 (2001), pp. 2127–2131.
[29] C.J. Smithells, *Metals Reference Book*, Elsevier, Chichester, 2013.
[30] U. Bohnenkamp, R. Sandström, and G. Grimvall, *Electrical resistivity of steels and face-centered-cubic iron*. J. Appl. Phys. 92 (2002), pp. 4402–4407.
[31] M. Ščepanskis, A. Jakovičs, I. Kaldre, W. Holweger, B. Nacke, and A.M. Diederichs, *The numerical model of electrothermal deformations of carbides in bearing steel as the possible cause of white etching cracks initiation*. Tribol. Lett. 59 (2015), p. 37.
[32] Z.Q. Lv, W.T. Fu, S.H. Sun, X.H. Bai, Y. Gao, Z.H. Wang, and P. Jiang, *First-principles study on the electronic structure, magnetic properties and phase stability of alloyed cementite with Cr or Mn*. J. Magn. Magn. Mater. 323 (2011), pp. 915–919.

[33] M.A. Konyaeva and N.I. Medvedeva, *Electronic structure, magnetic properties, and stability of the binary and ternary carbides (Fe,Cr)3C and (Fe,Cr)7C3*. Phys. Solid State 51 (2009), pp. 2084–2089.
[34] J. Languillaume, G. Kapelski, and B. Baudelet, *Cementite dissolution in heavily cold drawn pearlitic steel wires*. Acta Mater. 45 (1997), pp. 1201–1212.
[35] X. Sauvage, J. Copreaux, F. Danoix, and D. Blavette, *Atomic-scale observation and modelling of cementite dissolution in heavily deformed pearlitic steels*. Philos. Mag. A 80 (2000), pp. 781–796.
[36] C.A. Johnson, *Generalization of the Gibbs-Thomson equation*. Surf. Sci. 3 (1965), pp. 429–444.
[37] E. McEniry, R. Drautz, and G. Madsen, *Environmental tight-binding modeling of nickel and cobalt clusters*. J. Phys. Condens. Matter. 25 (2013), p. 115502.
[38] E. McEniry, T. Hickel, and J. Neugebauer, *Hydrogen behaviour at twist {110} grain boundaries in α -Fe*. Philos. Trans. R. Soc. Lond. A Math. Phys. Eng. Sci. 375 (2017), p. 20160402.
[39] G.A. Nematollahi, B. Grabowski, D. Raabe, and J. Neugebauer, *Multiscale description of carbon-supersaturated ferrite in severely drawn pearlitic wires*. Acta Mater. 111 (2016), pp. 321–334.
[40] H.B. Huntington and A.R. Grone, *Current-induced marker motion in gold wires*. J. Phys. Chem. Solids 20 (1961), pp. 76–87.
[41] V. V. Levitin, *Atom Vibrations in Solids: Amplitudes and Frequencies*, Cambridge Scientific Publishers, United States, 2004.
[42] J. Waser and L. Pauling, *Compressibilities, force constants, and interatomic distances of the elements in the solid state*. J. Chem. Phys. 18 (1950), pp. 747–753.
[43] C. Jiang, B.P. Uberuaga, and S.G. Srinivasan, *Point defect thermodynamics and diffusion in Fe3C: a first-principles study*. Acta Mater. 56 (2008), pp. 3236–3244.
[44] J. Takahashi, K. Kawakami, and M. Ueda, *Atom probe tomography analysis of the white etching layer in a rail track surface*. Acta Mater. 58 (2010), pp. 3602–3612.
[45] J. Takahashi, M. Kosaka, K. Kawakami, and T. Tarui, *Change in carbon state by low-temperature aging in heavily drawn pearlitic steel wires*. Acta Mater. 60 (2012), pp. 387–395.
[46] Y.J. Li, P. Choi, C. Borchers, S. Westerkamp, S. Goto, D. Raabe, and R. Kirchheim, *Atomic-scale mechanisms of deformation-induced cementite decomposition in pearlite*. Acta Mater. 59 (2011), pp. 3965–3977.
[47] Y. Li, D. Raabe, M. Herbig, P.-P. Choi, S. Goto, A. Kostka, H. Yarita, C. Borchers, and R. Kirchheim, *Segregation stabilizes nanocrystalline bulk steel with near theoretical strength*. Phys. Rev. Lett. 113 (2014), p. 106104.
[48] X. Sauvage and Y. Ivanisenko, *The role of carbon segregation on nanocrystallisation of pearlitic steels processed by severe plastic deformation*. J. Mater. Sci. 42 (2007), pp. 1615–1621.
[49] H. Hertz, *Ueber die Berührung fester elastischer Körper*. J. die Reine Angew. Math. 1882 (92) (1882), p. 156.
[50] A.V. Korznikov, Y.V. Ivanisenko, D.V. Laptionok, I.M. Safarov, V.P. Pilyugin, and R.Z. Valiev, *Influence of severe plastic deformation on structure and phase composition of carbon steel*. Nanostruct. Mater. 4 (1994), pp. 159–167.
[51] W.J. Nam, C.M. Bae, S.J. Oh, and S.-J. Kwon, *Effect of interlamellar spacing on cementite dissolution during wire drawing of pearlitic steel wires*. Scr. Mater. 42 (2000), pp. 457–463.
[52] D. Kalish and M. Cohen, *Structural changes and strengthening in the strain tempering of martensite*. Mater. Sci. Eng. 6 (1970), pp. 156–166.

[53] A.H. Cottrell and B.A. Bilby, *Dislocation theory of yielding and strain ageing of Iron*. Proc. Phys. Soc. London, Sect. A 62 (1949), pp. 49–62.
[54] D.E. Jiang and E.A. Carter, *Carbon dissolution and diffusion in ferrite and austenite from first principles*. Phys. Rev. B 67 (2003), p. 214103.
[55] A.D. Richardson, M.H. Evans, L. Wang, R.J.K. Wood, and M. Ingram, *Thermal desorption analysis of hydrogen in non-hydrogen-charged rolling contact fatigue-tested 100Cr6 steel*. Tribol. Lett. 66 (2017), p. 4.
[56] M. Nagumo, K. Takai, and N. Okuda, *Nature of hydrogen trapping sites in steels induced by plastic deformation*. J. Alloys Compd. 293–295 (1999), pp. 310–316.
[57] Y.-S. Chen, H. Lu, J. Liang, A. Rosenthal, H. Liu, G. Sneddon, I. McCarroll, Z. Zhao, W. Li, A. Guo, and J.M. Cairney, *Observation of hydrogen trapping at dislocations, grain boundaries, and precipitates*. Science 367 (2020), p. 171.
[58] F. Wei and K. Tsuzaki, *Hydrogen trapping phenomena in martensitic steels*, in *Gaseous Hydrogen Embrittlement of Materials in Energy Technologies*, Gangloff Richard P., Somerday Brian P., eds., Woodhead Publishing, Cambridge, 2012. pp. 493–525.
[59] H.K. Birnbaum and P. Sofronis, *Hydrogen-enhanced localized plasticity—a mechanism for hydrogen-related fracture*. Mat. Sci. Eng. A 176 (1994), pp. 191–202.
[60] R.A. Oriani, *Whitney award lecture – 1987: hydrogen – the versatile embrittler*. Corrosion 43 (1987), pp. 390–397.